

NLO QCD corrections to diphoton-plus-jet production through gluon fusion at the LHC

Ryan Moodie

Institute for Particle Physics Phenomenology
Durham University

Cavendish HEP seminars

1 Feb 2022

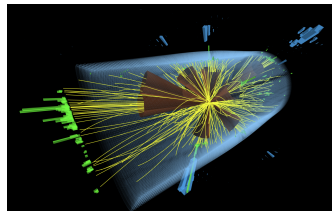


Precision frontier

- Precision QCD
 - Indirect probe of new physics by small deviations from SM
- Modern collider experiments demand increasing precision
- Percent-level QCD theory predictions
- Requires NNLO

$$\alpha_s \approx 0.1$$

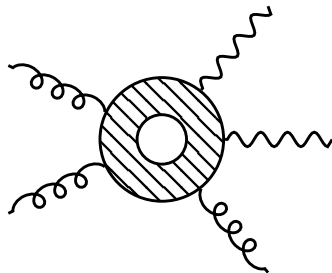
$$d\sigma = d\sigma^{\text{LO}} + \alpha_s d\sigma^{\text{NLO}} + \alpha_s^2 d\sigma^{\text{NNLO}}$$



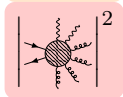
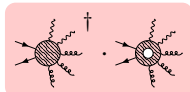
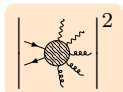
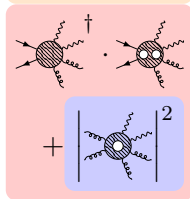
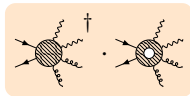
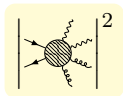
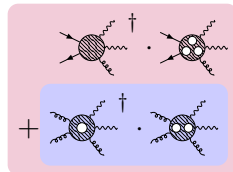
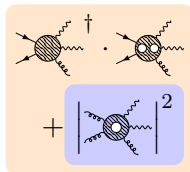
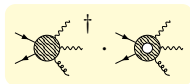
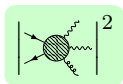
CMS

Diphoton final states

- Important background for measuring properties of the Higgs
 - Rich kinematics of $2 \rightarrow 3$ offer attractive probes
- Gluon-initiated channel is excellent testing ground for new technologies
 - Loop-induced
 - Simpler pole structure
 - Challenges conventional phase space optimisations
 - Simpler colour structure
- NNLO $pp \rightarrow \gamma\gamma j$ convergence slowest where gluon-fusion dominant [Chawdhry et al. 2021]



Perturbative expansion

 α_s^1 α_s^2 α_s^3 α_s^4

$$gg \rightarrow \gamma\gamma g + X$$

Outline

NLO QCD corrections to $gg \rightarrow \gamma\gamma g$

Virtual correction

NLO cross-section

Amplitude neural networks

Outline

NLO QCD corrections to $gg \rightarrow \gamma\gamma g$

Virtual correction

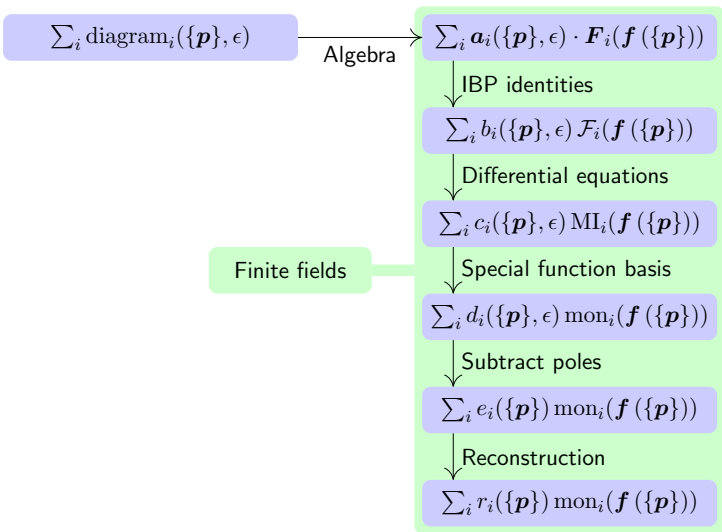
NLO cross-section

Amplitude neural networks

Virtual QCD corrections to $gg \rightarrow \gamma\gamma g$ amplitude

- Major theoretical challenge
- [Badger, Brønnum-Hansen, et al. 2021]
- Analytic 5-point 2-loop full-colour amplitudes
- Reconstruct over finite fields
- Pentagon function basis
- Fast and stable C++ implementation provided in NJet library
<https://bitbucket.org/njet/njet>

Computing loop corrections



Amplitude decomposition

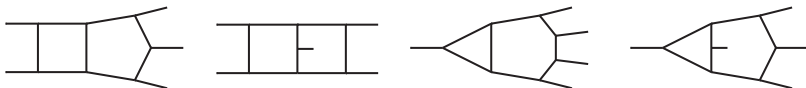
- Loops, helicity, colour

$$\mathcal{A}(1_g, 2_g, 3_g, 4_\gamma, 5_\gamma) = g_s g_e^2 \sum_{q=1}^{N_f} Q_q^2 \sum_{\ell=1}^{\infty} \left(n_\epsilon \frac{\alpha_s}{4\pi} \right)^\ell \sum_{h_i \in \{-, +\}} f^{a_1 a_2 a_3} A^{(\ell)}(1_g^{h_1}, 2_g^{h_2}, 3_g^{h_3}, 4_\gamma^{h_4}, 5_\gamma^{h_5})$$

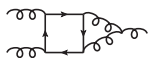
- Powers of N_c and N_f

$$\begin{aligned} A^{(1)}(1_g, 2_g, 3_g, 4_\gamma, 5_\gamma) &= A_1^{(1)}(1_g, 2_g, 3_g, 4_\gamma, 5_\gamma) \\ A^{(2)}(1_g, 2_g, 3_g, 4_\gamma, 5_\gamma) &= N_c A_1^{(2)}(1_g, 2_g, 3_g, 4_\gamma, 5_\gamma) + \\ &\quad \frac{1}{N_c} A_2^{(2)}(1_g, 2_g, 3_g, 4_\gamma, 5_\gamma) + \\ &\quad N_f A_3^{(2)}(1_g, 2_g, 3_g, 4_\gamma, 5_\gamma) \end{aligned}$$

Integral topologies



- 4 independent integral families
- Only LC contains non-planar integrals
 - Opposite pattern to quark-initiated channels
 - See by attaching photons to 3-gluon diagrams



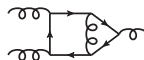
$$N_c$$



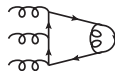
$$N_c$$



$$N_c$$



$$\frac{1}{N_c}$$



$$N_c - \frac{1}{N_c}$$

Finite fields

- Algebraic complexity: large intermediate expressions
- Bypass with numerical evaluation over finite fields \mathbb{F}_p

$$n \rightarrow n \bmod p$$

- Integer obtained by Chinese Remainder Theorem
- Use rational numbers modulo large prime numbers

$$r = \frac{a}{b} \rightarrow r \bmod p = (a \times (b^{-1} \bmod p)) \bmod p$$

- Avoids catastrophic cancellation of float
- FiniteFlow [Peraro 2019]
- Momentum twistor variables

Reconstruction

- Linear relations in r_i
 - Permutations of $5g$ coefficients as ansätze
- Univariate partial fraction decomposition
 - Needs no knowledge of analytic form
 - On the fly
 - Simplifies reconstruction
 - $\times 10$ point evaluation time
 - $\times \frac{1}{100}$ samples required
- Compact analytic expressions
 - Lowered polynomial degree

Implementation

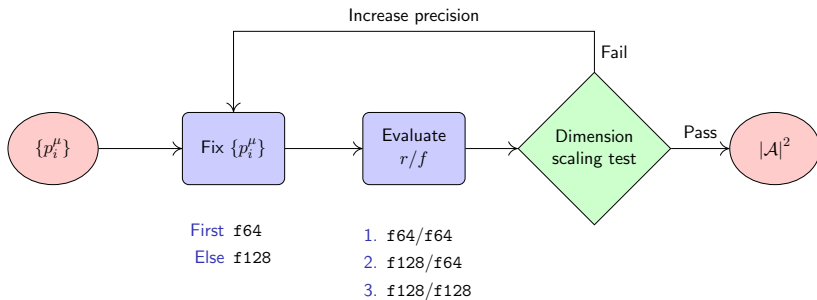
- Finite remainders coded up in NJet
 - Special functions from `PentagonFunctions++`
 - Sparse matrix algebra by `Eigen`
 - Extended precision through QD
- 6 independent helicity amplitudes analytically permuted to 16 mostly-plus helicities
- Construct partial amplitudes as

$$F^h = r_i^h(\boldsymbol{x}) M_{ij}^h f_j^h$$

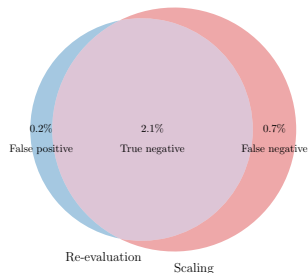
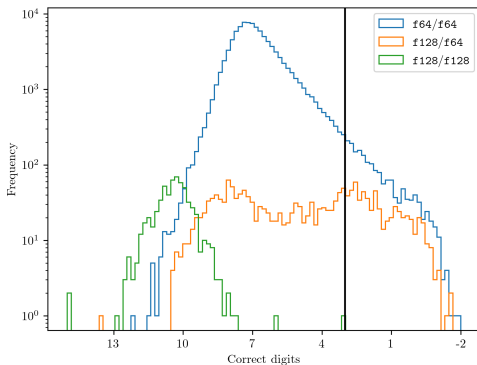
f_j^h	indexes pentagon function monomial list	global
M_{ij}^h	rational sparse matrices	partials
r_i^h	independent rational coefficients	helicities
\boldsymbol{x}	momentum twistor variables	global

- Mostly-minus configurations by complex conjugation of coefficients and parity flipping special functions

Evaluation strategy



Stability and test validation



Negative test results

- Compare direct f_{128}/f_{128} to strategy with 3 digit cutoff
- 60 000 points over NNLOJET one-loop phase space
- Most false positives have true error near cut: effect small
- Always anomalies in extreme phase spaces

Timing

- Evaluate over 100 000 points of “physical” phase space
- Mean timing per phase space point:
 - f64/f64: 9 s
 - 99 % of time on special functions
 - Evaluation strategy with three digit target: 26 s
- *Ready for phenomenology*
 - Stability
 - Efficiency

Outline

NLO QCD corrections to $gg \rightarrow \gamma\gamma g$

Virtual correction

NLO cross-section

Amplitude neural networks

NLO QCD correction to $gg \rightarrow \gamma\gamma g$ cross-section

- [Badger, Gehrmann, et al. 2022]
- First differential cross sections from 5-point 2-loop full-colour amplitudes for the LHC
- Although N³LO in $pp \rightarrow \gamma\gamma j$, large gluon PDF amplifies contribution
- Observe significant NLO corrections
- Important ingredient to be combined with NNLO $pp \rightarrow \gamma\gamma j$

NLO construction

$$\begin{aligned}
 \sigma_{gg \rightarrow \gamma\gamma g + X}^{\text{NLO}} = & \int d\Phi_3 \left| \text{diagram}_1 \right|^2 + \\
 & \int d\Phi_3 2 \text{Re} \left(\text{diagram}_1^\dagger \cdot \text{diagram}_2 \right) + \\
 & \int d\Phi_4 \left| \text{diagram}_3 \right|^2 + \int d\Phi_4 \left| \text{diagram}_4 \right|^2 + \mathcal{O}(\alpha_s^5)
 \end{aligned}$$

The diagrams represent Feynman diagrams for the process $gg \rightarrow \gamma\gamma g + X$. Diagram 1 is a tree-level diagram with a quark loop. Diagram 2 is a tree-level diagram with a quark loop and a photon emission from the internal quark line. Diagram 3 is a tree-level diagram with a quark loop and a photon emission from the external quark line. Diagram 4 is a tree-level diagram with a quark loop and a photon emission from the external quark line.

(γ couple to internal quark loop)

Amplitudes

- $\mathcal{A}_V^{(2)}$ from NJet (section 2)
 - 3 digit accuracy threshold
- $\mathcal{A}^{(1)}$ for LO and R from combination of OpenLoops2 [Buccioni et al. 2019] and NJet
 - OpenLoops2 generally more efficient
 - NJet necessary for high precision evaluation of exceptional points

Infrared regularisation

- $\mathcal{A}_{\text{LO}}^{(1)}$ and $\mathcal{A}_{\text{R}}^{(1)}$ finite since loop-induced
- Renormalised $\mathcal{A}_{\text{V}}^{(2)}$ IR divergent from loop integration
- σ^{R} IR singular for unresolved emissions
- Cancel by KLN theorem
- Use finite remainder of \mathcal{A}_{V}
- Cancel with antenna subtraction method [Currie, Glover, and Wells 2013]

Cuts

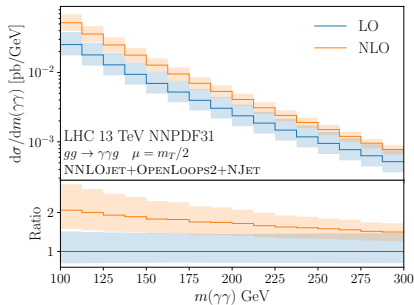
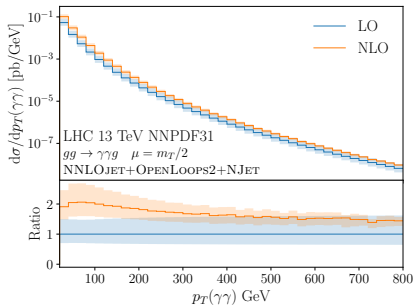
Cuts are typical for 13 TeV LHC

- $p_T(\gamma_1) > 30 \text{ GeV}$
- $p_T(\gamma_2) > 18 \text{ GeV}$
- $|\eta(\gamma\gamma)| < 2.4$
- $m(\gamma\gamma) \geq 90 \text{ GeV}$
- $p_T(\gamma\gamma) > 20 \text{ GeV}$
- $\Delta R_{\gamma\gamma} > 0.4$
- Photons selected by smooth cone isolation
 - $\Delta R_0 = 0.4$
 - $E_T^{\text{max}} = 10 \text{ GeV}$
 - $\epsilon = 1$
- No jet requirement as $p_T(\gamma\gamma)$ cut avoids all outgoing partons unresolved

Details

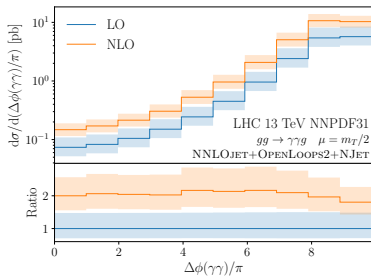
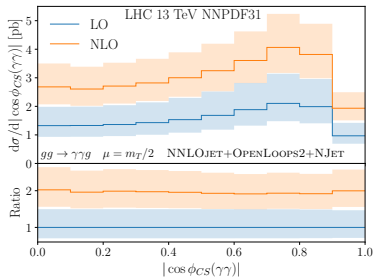
- Parameters
 - PDFs: NNLO set of NNPDF3.1
 - α_s evaluated using LHAPDF with $\alpha_s(m_Z) = 0.118$
 - $\alpha = 1/137.035999139$
- Chosen for comparison with full NNLO [Chawdhry et al. 2021]
- Uncertainties
 - MC errors $< 1\%$ (not on plots)
 - Theory uncertainty from 7-point variation around dynamical central value:
 - $\mu_F = \mu_R = \mu = \frac{1}{2}m_T = \frac{1}{2}\sqrt{m^2(\gamma\gamma) + p_T^2(\gamma\gamma)}$

Distributions 1



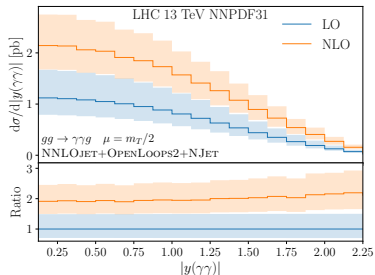
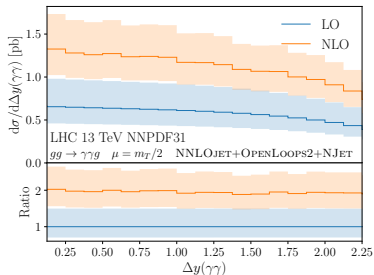
- NLO corrections often comparable in size to LO
- Corrections largest at low $p_T(\gamma\gamma)$ and $m(\gamma\gamma)$
- Smoothly decreasing from 2 towards 1.5

Distributions 2



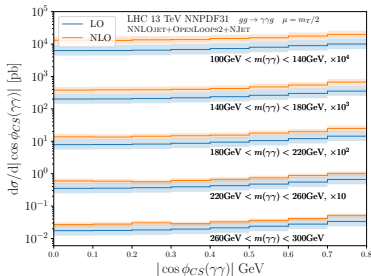
- Distributions differential only in geometrical photon variables
 - Collins-Soper angle, azimuthal decorrelation
- Total cross section dominated by low $p_T(\gamma\gamma)$ or $m(\gamma\gamma)$
- Near-uniform ratio of 2
- No overlap of uncertainties

Distributions 3

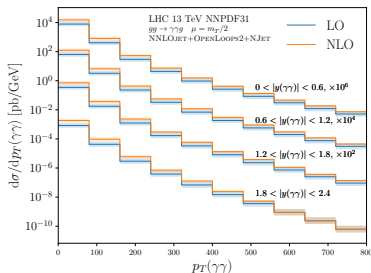


- Distributions differential only in geometrical photon variables
 - Rapidity different, total rapidity
- LO and NLO absolute scale uncertainties appear comparable
- Relative uncertainty reduced from 50% at LO to 30% at NLO

Doubly-differential distributions 1

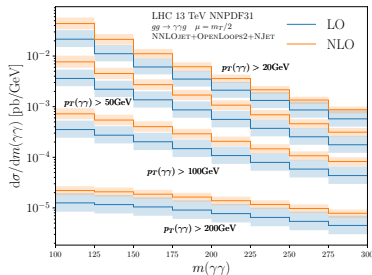
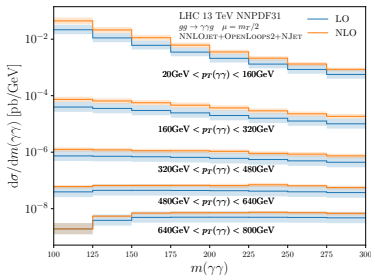


- NLO/LO decreasing with $m(\gamma\gamma)$
- Uniform in $|\phi_{CS}(\gamma\gamma)|$



- NLO/LO decreasing with $p_T(\gamma\gamma)$
- More pronounced at forward rapidity than central

Doubly-differential distributions 2



- Non-uniform shape in highest p_T bin
- Logarithmic corrections in $\log(m(\gamma\gamma)/p_T(\gamma\gamma))$

Takeaway

- *Significant NLO corrections*
- Inclusion into full NNLO diphoton-plus-jet will further enhance predictions at low $p_T(\gamma\gamma)$ and $m(\gamma\gamma)$
- Demonstrates importance of combining gluon-induced and quark-induced diphoton-plus-jet signatures for LHC

Outline

NLO QCD corrections to $gg \rightarrow \gamma\gamma g$

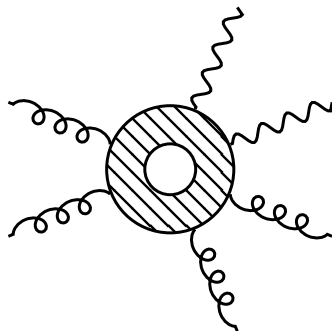
Virtual correction

NLO cross-section

Amplitude neural networks

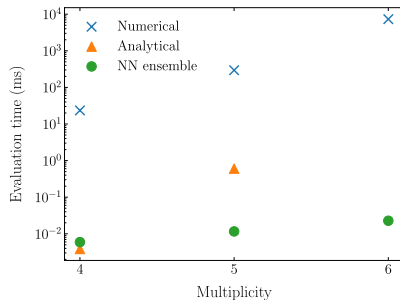
Amplitude neural networks for $gg \rightarrow \gamma\gamma + \text{jets}$

- Approximate matrix elements with neural networks
 - Train models using amplitude libraries
 - Tame IR behaviour
 - Apply in realistic hadronic collider simulations
- Applicable to real correction of $gg \rightarrow \gamma\gamma$
 - Computational bottleneck
- [Aylett-Bullock, Badger, and Moodie 2021]
- https://gitlab.com/JosephPB/n3jet_diphoton



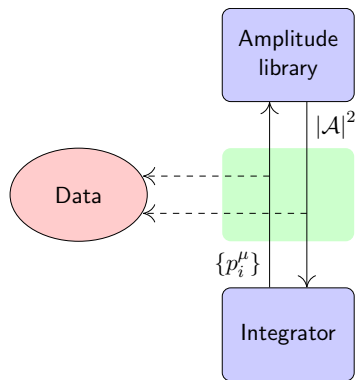
Amplitudes

- Loop-induced
 - Challenge conventional event generator optimisations
- Use amplitudes from NJet
- Numerical
 - Integrand reduction, generalised unitarity
 - Automated but slow
- Analytical
 - High multiplicity unavailable
- Amplitude neural network (ANN)
 - Favourable time scaling



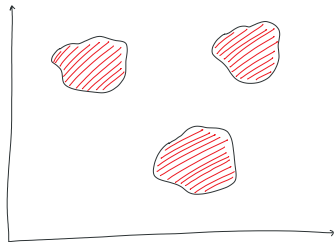
Data generation

- Extract from integrator
- First run
 - 100k points
 - 4:1 training and validation sets
- Second run
 - 3M points
 - Testing with different random number seed
- Standardise input and output variable distributions
 - Mean of 0
 - Standard deviation of 1



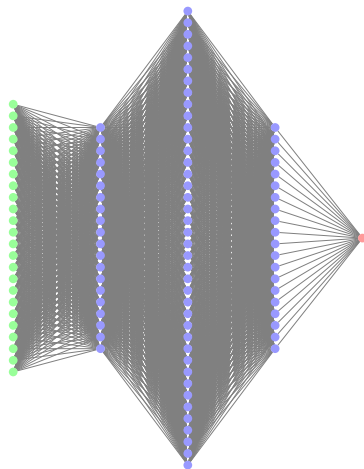
Phase-space partitioning

- IR divergences from soft s_i and collinear c_{ij} emissions
- Naive model struggles
- Partition phase space
 - \mathcal{R}_{div} and $\mathcal{R}_{\text{non-div}}$
 - Cut on $\min(s_{ij}/s_{12})$
- Sub-divide \mathcal{R}_{div} using FKS
 - $\mathcal{P}_{\text{FKS}} = \{(i, j) \mid s_i \vee s_j \vee c_{ij}\}$
 - $\mathcal{S}_{ij} = 1 / \left(s_{ij} \sum_{j,k \in \mathcal{P}_{\text{FKS}}} \frac{1}{s_{jk}} \right)$
 - Partition functions smoothly isolate singularities
 - $|\mathcal{A}|^2 = \sum_{i,j \in \mathcal{P}_{\text{FKS}}} \mathcal{S}_{ij} |\mathcal{A}|^2$
 - Weighted network for each \mathcal{S}_{ij}
- [Badger and Bullock 2020]



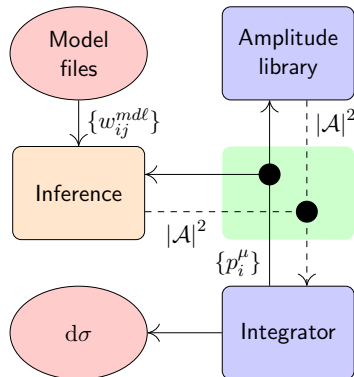
Model architecture

- General architecture
 - Ensemble, partition, process, cuts
 - Hyperparameter optimisation on $gg \rightarrow \gamma\gamma g$
- Fully-connected neural network
 - Keras with TensorFlow backend
 - $n \times 4$ input nodes
 - 20-40-20 hidden nodes (hyperbolic-tangent)
 - Single output node (linear)
- Training by gradient descent
 - Mean-squared-error loss function
 - Adam optimisation
 - Training epochs by Early Stopping



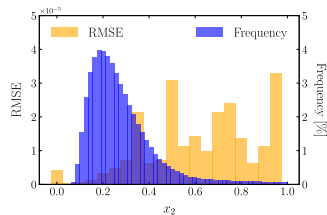
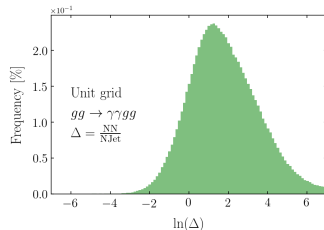
Interfacing with event generators

- Infer on ensemble of 20 models
 - Different random weight initialisation
 - Shuffled data sets
 - Mean and standard error (precision/optimalty errors)
- Training in Python
 - Event generators in C++
- C++ inference code
 - Linear algebra by Eigen
- C++ interface with Sherpa
- LHAPDF, NNPDF31_nlo_as_0118, Rivet

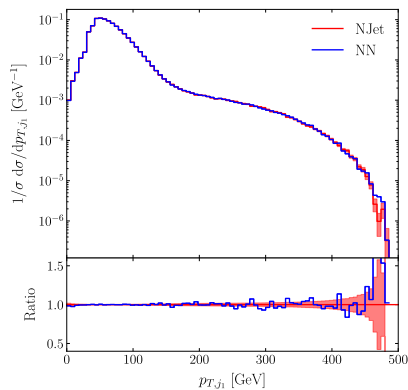
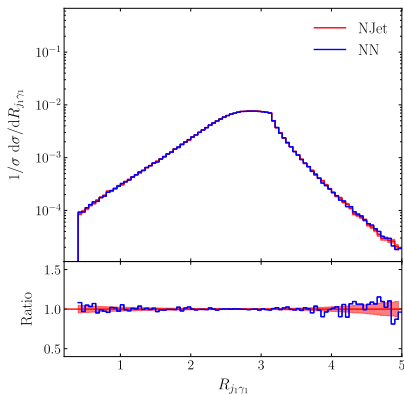


Per-point agreement between ANN and NJet

- Gaussian error distribution
 - Shifted mean
- IR regions difficult to fit
- Gluon PDF suppresses these errors
- Total cross section in agreement
 - $\sigma_{\text{NN}} = (4.5 \pm 0.6) \times 10^{-6} \text{ pb}$
 - $\sigma_{\text{NJet}} = (4.9 \pm 0.5) \times 10^{-6} \text{ pb}$
- Improved tree-level descriptions using factorisation
 - [Maître and Truong 2021]



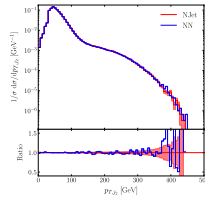
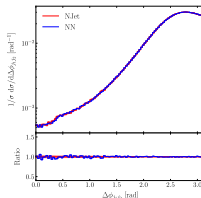
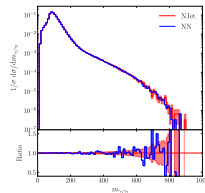
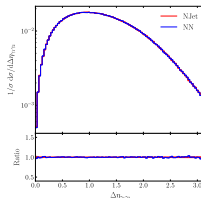
Distributions $gg \rightarrow \gamma\gamma gg$



Excellent agreement

Summary

- Extend pioneering work on ANNs to full hadronic collider simulations
 - Loop-induced $gg \rightarrow \gamma\gamma + \text{jets}$
 - FKS partitioned phase space
 - Provide interface to Sherpa
- *ANNs provide general framework for optimising high-multiplicity observables*
 - Excellent agreement in distributions
 - Simulation speed-up: $N_{\text{infer}}/N_{\text{train}}$



Outline

NLO QCD corrections to $gg \rightarrow \gamma\gamma g$

Virtual correction

NLO cross-section

Amplitude neural networks

Conclusion

- NLO QCD corrections to diphoton-plus-jet production through gluon fusion
 - Well motivated for LHC phenomenology
 - Success of advances in QCD theory
- Complete 2-loop full-colour finite remainder
 - Efficient and stable evaluation over physical scattering region
- Fully differential distributions in NLO cross-section
 - Significant NLO corrections
 - Important contribution for precision studies of diphoton-plus-jet production
- ANNs provide general framework to optimise high-multiplicity observables
 - Applicable to real correction of $gg \rightarrow \gamma\gamma g$

Bibliography



Aylett-Bullock, Joseph, Simon Badger, and Ryan Moodie (Aug. 2021). "Optimising simulations for diphoton production at hadron colliders using amplitude neural networks". In: *Journal of High Energy Physics* 2021.66. ISSN: 1029-8479. DOI: 10.1007/JHEP08(2021)066. arXiv: 2106.09474 [hep-ph].



Badger, Simon, Christian Brønnum-Hansen, et al. (Nov. 2021). "Virtual QCD corrections to gluon-initiated diphoton plus jet production at hadron colliders". In: *Journal of High Energy Physics* 2021.83. ISSN: 1029-8479. DOI: 10.1007/JHEP11(2021)083. arXiv: 2106.08664 [hep-ph].



Badger, Simon and Joseph Bullock (2020). "Using neural networks for efficient evaluation of high multiplicity scattering amplitudes". In: *JHEP* 06, p. 114. DOI: 10.1007/JHEP06(2020)114. arXiv: 2002.07516 [hep-ph].



Badger, Simon, Thomas Gehrmann, et al. (Jan. 2022). "Next-to-leading order QCD corrections to diphoton-plus-jet production through gluon fusion at the LHC". In: *Physics Letters B* 824, p. 136802. ISSN: 0370-2693. DOI: 10.1016/j.physletb.2021.136802. arXiv: 2109.12003 [hep-ph].



Buccioni, Federico et al. (2019). "OpenLoops 2". In: *Eur. Phys. J. C* 79, p. 866. DOI: 10.1140/epjc/s10052-019-7306-2. arXiv: 1907.13071 [hep-ph].



Chawdhry, Herschel A. et al. (2021). "NNLO QCD corrections to diphoton production with an additional jet at the LHC". In: arXiv: 2105.06940 [hep-ph].



Currie, James, E. W. N. Glover, and Steven Wells (2013). "Infrared Structure at NNLO Using Antenna Subtraction". In: *JHEP* 04, p. 066. DOI: 10.1007/JHEP04(2013)066. arXiv: 1301.4693 [hep-ph].



Maître, Daniel and Henry Truong (2021). "A factorisation-aware Matrix element emulator". In: *JHEP* 11, p. 066. DOI: 10.1007/JHEP11(2021)066. arXiv: 2107.06625 [hep-ph].



Peraro, Tiziano (2019). "FiniteFlow: multivariate functional reconstruction using finite fields and dataflow graphs". In: *JHEP* 07, p. 031. DOI: 10.1007/JHEP07(2019)031. arXiv: 1905.08019 [hep-ph].